Lithuanian Journal of Physics, Vol. **55**, No. 2, pp. 84–91 (2015)

CLASSIFICATION OF THE $5p^5$*nln'l' LSJ* ENERGY LEVELS OF Cs EXCITED BY 30 eV ELECTRONS

G. Kerevičius and A. Kupliauskienė

Institute of Theoretical Physics and Astronomy of Vilnius University, A. Goštauto 12, LT-01108 Vilnius, Lithuania
E-mail: alicija.kupliauskiene@tfai.vu.lt; gintaras.kerevicius@tfai.vu.lt

Received 27 January 2015; accepted 20 March 2015

Theoretical investigation of the $5p^5nl(L_1S_1)n'l'$ *LSJ* autoionizing states of Cs was performed by using large scale configuration interaction calculations of energy levels, autoionization probabilities and excitation cross sections obtained in the Dirac–Fock–Slater approximation. Classification of calculated energy levels in the *LSJ* coupling scheme of angular momenta and simulation of the intensities of ejected Auger electron spectrum were performed. The classified energy levels in the region from the excitation threshold up to 17.365 eV and simulated intensity spectrum were used for identification of the experimental ejected-electron spectrum of Cs excited by 30 eV electrons.

Keywords: electronic structure of atoms and molecules: theory, autoionization, atomic excitation and ionization

PACS: 31.15.-p, 32.80.Zb, 34.80.Dp

1. Introduction

Theoretical investigation of the 5p-core-excited autoionizing states of Cs is a complex task as the relativistic effects play a more important role compared with Na [1, 2, 3, 4], K [5] or Rb [6]. The first attempt to perform the classification of Cs spectrum registered in an ultraviolet absorption experiment was made by Connerade [7] in *jK* notations. As the lower series members did not conform to the *jK* coupling, new observations of the synchrotron radiation absorption spectrum were classified by using the *LSJ* coupling scheme [8]. Intermediate coupling Hartree–Fock calculations without configuration mixing were performed for the 5p-excited $6s^2$, 5d6s, 6s7s and $5d^2$ configurations [8]. It was found that the accuracy was insufficient to perform assignments around $Z = 56$, but the results were used to estimate the energies of the most important 5p-excited levels. Calculations of excitation energies, cross sections, radiative and autoionization probabilities for the states of the $5p^56s^2$, $5p^55d6s$, $5p^56s6p$ and $5p^56s7s$ lowest autoionizing configurations were performed in [9] by using the Dirac–Fock–Slater [10] approximation. In the case of odd states, a superposition of the $5p^56s^2$, $5p^55d6s$ and $5p^56s7s$ was used. Superposition of the $5p^66s$ and $5p^56s6p$ configurations was used for the even states. Calculated energy levels and excitation cross sections were applied for the identification of experimental spectra [9]. Large scale configuration interaction calculations of energy levels, autoionization probabilities and 400 eV electron-impact excitation cross sections of the $5p^5$*nln'l' LSJ* (*nl* = 5d, 6s; *n'l'* = 5d, 6(s–d), 7(s, p), 8s) autoionizing states of Cs were performed for the first time in [11]. The relativistic effects were taken into account using the Dirac–Fock–Slater approximation [10]. The calculated data were used for a novel identification of 37 lines of the experimental ejected-electron spectrum [12] excited by 400 eV electrons. But, a total of 63 Cs I levels were observed in [12] by using an electron beam of 30, 50 and 400 eV incident energy. The spectra at 30 and 50 eV are rich of lines compared with that at 400 eV. Theoretical data from [11] were also used for a new assignment of the line at 14.208 eV [12] as $5p^56s^2\ ^2P_{1/2}$ [13]. Revised identification of the experimental spectrum [12] was performed for low energy Auger lines and presented in [14].

The energy levels of $5p^5$*nln'l'* configurations of Cs were calculated in the *jjJ* coupling scheme of angular momenta. The coupling of each energy level was then transformed from *jjJ* to *LSJ*. Expansion coefficients of the *LSJ* coupling scheme were presented in [11], but rigorous theoretical classification of levels was not performed. The main task of the present work is to perform a revised classification of the calculated energy levels using the *LSJ* coupling scheme, simulate a theoretical intensity spectrum of the levels, and apply both for a more accurate and full identification of the experimental spectrum excited by 30 eV electrons [12].

2. Method of calculations

Expansion coefficients of the *LSJ* coupling scheme were used from [11] to classify the calculated energy levels. New calculations of energies, autoionization probabilities and electron-impact excitation cross sections more suitable for simulation of the intensities of ejected Auger electron spectrum were performed in the basis of mixed relativistic configurations by using the Flexible Atomic Code [10]. The radial orbitals for construction of basis states were derived from a modified self-consistent Dirac–Fock–Slater iteration on the fictitious mean configuration with fractional occupation numbers representing an average electron cloud of configurations included in the calculation. In order to optimize the local central potential including the approximated exchange part, the configuration $5p^6 6s$ was used. The following singly-excited and 5p-core-excited configurations were used to take into account the correlation effects as well: $5p^6 nl$, nl = (4, 5)f, (7–12) (s–d); $5p^5 nln'l'$, nl = (4, 5)f, (5–7)d, (6–8) (s, p, f); $n'l'$ = (4–8)f, 5d, (6–11)(s–d). Since the local potential was optimized only for the ground state, to reduce the errors on total energies the following correction procedure was applied. Before the potential for the mean configuration with fractional occupation numbers was calculated, the optimized potential for each configuration was obtained, and the average energy of each configuration was calculated by using this potential. Then, the average energy for each configuration was calculated with the potential optimized for the mean configuration with fractional occupation numbers. The difference of the two average energies was then applied as a correction to all states within each configuration after the Hamiltonian was diagonalized. The total number of both odd and even states included in the calculation was 12487. The electron-impact excitation cross sections and autoionization probabilities were calculated in the relativistic distorted-wave approximation [10] by using the same basis set.

The intensity of the line of emitted Auger electrons from the electron-impact excited state αLSJ is [15, 16]

$$I(\alpha LSJ,\theta) \sim \frac{\mathrm{d}\sigma(\alpha LSJ,\theta)}{\mathrm{d}\theta} = B(\alpha LSJ)\frac{\sigma(\alpha LSJ)}{4\pi}\left[1+\sum_{K>0,\,\mathrm{even}}^{2J}\beta_K \mathrm{P}_K(\cos\theta)\right], \qquad (1)$$

where $\mathrm{d}\sigma(\alpha LSJ,\theta)/\mathrm{d}\theta$ is the polar angle θ dependent differential cross section, $\sigma(\alpha LSJ)$ is the total excitation cross section of the state αLSJ, $\mathrm{P}_K(\cos\theta)$ is the Legendre polynomial of rank K, and $B(\alpha LSJ)$ is the Auger electron yield:

$$B(\alpha LSJ) = \frac{A^a(\alpha LSJ)}{\sum_i A_i^r(\alpha LSJ) + \sum_i A_i^a(\alpha LSJ)}. \qquad (2)$$

In the case when the radiative transition probabilities A^r_i from the state αLSJ to lower lying states i are much smaller than autoionization ones A^a_i and only one Auger decay channel exists, the Auger yield is very close to 1. Our calculations show that for the investigated autoionizing states of Cs the radiative transition probabilities are about 3 to 4 orders of magnitude smaller than autoionization ones, therefore they can be disregarded in Eq. (2). The asymmetry parameter $\beta_K = A_K\alpha_K$ [15] in Eq. (1) is a product of the alignment parameter A_K [16] due to an electron-impact excitation of an atom and the asymmetry parameter of the angular distribution of Auger electrons α_K [17] due to a spontaneous decay of the autoionizing state of the atom. For the magic angle $\theta = 54.7°$, $\mathrm{P}_2(\cos(54.7°)) \simeq 0$ and $\mathrm{P}_4(\cos(54.7°)) \simeq -0.39$, i. e. the Legendre polynomials of rank $K > 2$ are not equal to zero even for the magic angle. In addition, $A_K = 0$ for all $J = 1/2$ states of the excited atom. Therefore, intensity ratios of the $J = 1/2$ and $J > 1/2$ lines observed at 75° can differ significantly from the ratios obtained when we exclude the asymmetry of the angular distribution of ejected electrons (see details in [18] for the core-excited Rb).

3. Results and discussion

For **theoretical classification** of the $5p^5 nln'l'$ *LSJ* levels, the expansion coefficients from [11] were used. A simpler effective potential of the present calculation resulted in a relatively small change of the level energies (less than 0.13 eV) allowing us to keep the same assignments of *LSJ*. In the case of the autoionizing states of Cs, the *LSJ* coupling scheme of angular momenta is valid only for the lowest levels. Therefore, we have met some difficulties while performing theoretical classification for a number of higher energy states. For some of levels, the number of expansion coefficients presented in Table 1 [11] was insufficient for an unambiguous assignment of the *LSJ* quantum numbers. Then, other terms of the wave function were used from the original data [19]. The assignments for all levels starting from the lowest one $5p^5 6s^2\ {}^2P_{3/2}$ up to 15.451 eV are presented in Table 1. Table 2 is devoted to the levels from 15.463 eV up to 17.365 eV with excitation cross sections greater than 5×10^{-20} cm^2 in the case of 30 eV impacting electrons.

Comparison of the present and Table 2 [11] classification presented in Table 3 shows that in the present work it has changed for 13 levels. The change was made based on the three criteria, the first and the second being the absolute value and position of the expansion coefficient of an assigned state. For the third criterion, we have assumed that the states originating from the $5p^56s\ ^3P$ and $5p^55d\ ^3L$ (L = P, D, F) in the assignment should be lower than the $5p^56s\ ^1P$ and $5p^55d\ ^1L$ ones if the expansion coefficients are approximately equal, as it was in the case of K [5] and Rb [6]. Differences among the absolute values of expansion coefficients are small, therefore a condition for the unambiguous classification was used, i. e. not to attribute the same *LSJ* state to two levels in all calculated spectrum. Indicating by level energies in the current (and Table 2 of [11]) work, only the intermediate L_1S_1 term has changed for the 13.586 (13.650) eV, 14.790 (14.886) eV, 15.723 (15.810) eV and 15.732 (15.849) eV states. Only the final *LS* term has changed for the 15.117 (15.209) eV state, while both (L_1S_1) *LS* have changed for the states of 13.664 (13.797) eV and 13.908 (13.994) eV energy. For other 6 levels of 15.177 (15.289) eV, 15.306 (15.289) eV, 15.296 (15.378) eV, 16.411 (16.506) eV, 16.610 (16.711) eV and 17.072 (17.180) eV energy the configuration was revised. In later measurements by Mendelsohn et al. [20] the observed energy of 13.174 eV was assigned to the $5d(^3P)6s\ ^4P_{5/2}$ state, which is very close to the calculated energy of 13.127 eV in the present work (13.149 eV in [12]).

For some levels, a superposition of two or more eigenstates could be assigned unambiguously, e. g. for $J = {}^3/_2$ the expansion is $\{0.60 \cdot 5d(^3F)6s\ ^4F - 0.55 \cdot 5d(^1D)6s\ ^2D\}$ at 13.664 eV, $\{0.54 \cdot 6s(^1P)6p\ ^2D + 0.46 \cdot 6s(^3P)6p\ ^2P\}$ at 13.908 eV, or $\{0.42 \cdot 5d(^3D)6s\ ^2D + 0.35 \cdot 5d(^1P)6s\ ^2P\}$ at 14.790 eV energy of the present work. Notice that the second expansion coefficient of the 13.664 and 13.908 eV levels is the same as the first of Table 2 in [11], i. e. the actual assignment has not changed. However, the described feature applies only for these Table 2 [11] states. The same feature was observed in [13, 14] for the $\{5d^2(^3F)\ ^4D + 5d(^3P)6s\ ^2P\}_{1/2}$ of 14.072 eV [12] and $\{5d(^1P)6s\ ^2P + 5d(^3D)6s\ ^2D\}_{3/2}$ of 14.574 eV [12] states. There are more states for which the classification of two sets of quantum numbers could be attributed. For the sake of convenience, only one set of quantum numbers was left in Tables 1 and 2.

Influence of the asymmetry of Auger electron angular distribution was evaluated as measurements in [12] were performed at the angle of 75° with respect to the direction of incident electrons. In the case of 400 eV incident electrons, it was assumed in [11] that the asymmetry parameters β_K of the angular distribution of ejected electrons from electron-impact excited autoionizing states were close to zero. In the case of the autoionization from the $np^5n'l'n''l''$ *LSJ* states, only one $np^6\varepsilon\lambda$ *LSJ* decay channel is possible. Then, the matrix elements which depend on the radial part of wave function of the free electron (see Eq. (4) in [21]) cancel in the numerator and denominator of Eq. (10) [21], and the parameter α_K is equal to some constant, i. e. it does not depend on the energy of ejected electron. Therefore, β_K dependence on the energy is defined only by the alignment parameter A_K. The calculation of A_K for the Na [22] and K [22] state $np^5(n+1)s^2\ ^2P_{3/2}$ has shown that A_K was approaching zero when the energy of incoming electrons was increasing. The parameter $\alpha_2 = -1$ for the $np^5(n+1)s^2\ ^2P_{3/2}$ states [23]. Our calculations show that it is also equal to –1 for the $J = {}^3/_2$ states of 5p-excited $6s^2$, 5d6s and 6s6p configurations. But α_K parameters of the higher rank K are not, e. g. $\alpha_4 = 0.925$ for the state $5p^56s(^1P)6p\ ^2D_{5/2}$.

To evaluate the influence of A_K on the asymmetry parameter β_K for ejected electrons emitted at 75°, calculations for several autoionizing states of Cs were performed in the non-relativistic single configuration approximation by using our own computer codes. The radial wave functions and intermediate coupling expansion coefficients for atoms in discrete states were obtained in the Breit-Pauli approximation by using a complex of programs [24]. For the incident electron energy of 30 eV, the alignment parameter $A_2 = -0.27$ for $5p^56s^2\ ^2P_{3/2}$, $A_2 = -0.47$ for $5p^55d(^1P)6s\ ^2P_{3/2}$, $A_2 = -0.23$ for $5p^56s(^1P)6p\ ^2D_{3/2}$, $A_2 = -0.24$ and $A_4 = 0.22$ for $5p^56s(^1P)6p\ ^2D_{5/2}$. In the case of 400 eV impacting electrons, the same parameters are equal to –0.04, 0.05, 0.31, 0.33 and 0.14, respectively. It shows that the asymmetry of the angular distribution of Auger electrons excited by electron-impact could be strong, and it should be taken into account while performing the identification of a measured spectrum at low projectile energies. Thus, a conclusion follows up that it is not enough to take into account only the values of total excitation cross sections while performing the identification of a measured spectrum even in the case of high energies of impacting electrons.

Our calculations for excitation of the autoionizing states of Cs and Rb [18] have shown that the alignment parameters A_K depend strongly on the configuration and total angular momentum J, but are very similar for the total orbital L and spin S angular momenta. It is sufficient to calculate the factors $C = 1 + \sum_K A_K\alpha_K P_K(\cos\theta)$ only for the $5p^5nln'l'$ J states which are a good tool to estimate the change of ratios of the intensities of Auger lines in the case of $J = {}^1/_2$ and $J \geq {}^3/_2$. The C factors were calculated in the intermediate coupling single configuration approximation and are presented in Table 4 for the case of 30 eV impacting electrons. The factor is symmetric with respect to the half of the interval of 0° and 180° and has a minimum at 90°, therefore it is presented in Table 4 only up to 90°. It is equal to 1 for the states with $J = {}^1/_2$ as only $K = 0$ is possible. The values of C factors from Table 4 indicate that a differential cross section measured at the magic angle 54.7° for the $J > {}^3/_2$ states can decrease up to 20% compared with the case of $J = {}^3/_2$. The same decrease is bigger in the case of 75° and reaches 25% (see $J = {}^5/_2$ of the $5p^55d6s$ in Table 4).

Identification of experimental lines. To assign quantum numbers for the Auger lines in the spectrum registered by using 30 eV impacting electrons [12], the simulated spectrum is used. It is presented in Figure together with the experimental spectrum [12]. For the simulation of theoretical spectrum the convolution of Gaussian and natural line profiles was used. The Gaussian line width was 20 meV and the natural line width was calculated using the autoionization probabilities from the present work. Comparison of both spectra in the figure shows that some theoretical lines should be shifted to the lower energy region. For example, the theoretical line at 14.790 eV was shifted by –0.216 eV to coincide with the most intensive experimental line at 14.574 eV. The dependence of Auger lines on the energy of impacting electrons was also taken into account by comparing the intensities of both measured [12] and simulated spectra at 30 and 400 eV [11]. Decrease of the intensity of some lines due to the asymmetry of the angular distribution of Auger electrons (see Table 4) was also taken into account. The suggested identification is presented in Tables 1 and 2.

In the present work, the assignment of quantum numbers for 27 of 63 [12] observed states has suffered some changes compared with the identification presented in the previous works [11, 13]. Assignments were given to 24 lines for the first time. Based on our calculations the experimental line at 16.657 eV [12] could be assigned to the doublet state, which is between 16.359 and 16.411 eV states in the present calculation. The state is not presented in Table 2 for the reason mentioned in the beginning of this section. One of reasons for the change of an assignment was a revised classification of the calculated levels. Another reason is caused by the differences of the intensities of lines registered at 30 and 400 eV incident electron energy [12]. The doublet terms and dipole-forbidden terms, strongly mixed with doublet terms ($J = {}^1/_2, {}^3/_2$), give a large contribution to the total intensity of Auger lines at 400 eV, whereas the energy of 30 eV impacting electrons is close to the excitation threshold of the 5p-core-excited states of Cs. Therefore, the quartet and other dipole-forbidden terms ($J > {}^3/_2$) have the largest intensities. The dipole-allowed transitions, which dominate in the 400 eV spectrum [11, 12], are blended by lines from the dipole-forbidden states in the 30 eV spectrum (see Fig. 1 in [11] and Figure for comparison). For example, the experimental lines observed in [12] were reassigned (in [11] → in the present work) to the states: $5d(^3P)6s\ ^2P_{1/2} \rightarrow 5d(^3P)6s\ ^4P_{5/2}$, $6s(^1P)6p\ ^2D_{3/2} \rightarrow 5d(^3F)6s\ ^4F_{7/2}$, $5d(^1D)6s\ ^2D_{3/2} \rightarrow 6s(^3P)6p\ ^4D_{5/2}$, $5d(^3P)6p\ ^2P_{1/2} \rightarrow 5d^2(^3F)\ ^4D_{7/2}$, at 13.149 eV, 13.344 eV, 13.600 eV and 14.476 eV, respectively. A corresponding number of the calculated levels presented in Tables 1 and 2 up to 17.365 eV was used to identify all 63 experimental lines observed in [12]. The state at 17.365 eV is the 1203th of 12487 states included in the calculation. For the reason mentioned in the first paragraph of this section, 8 and 896 energy levels were not included in the left and right parts of Table 2, respectively. All not included levels and the levels starting from 17.365 eV could be useful for identification of the spectra measured with impacting electrons of an intermediate or higher energy, e. g. 50–70 eV.

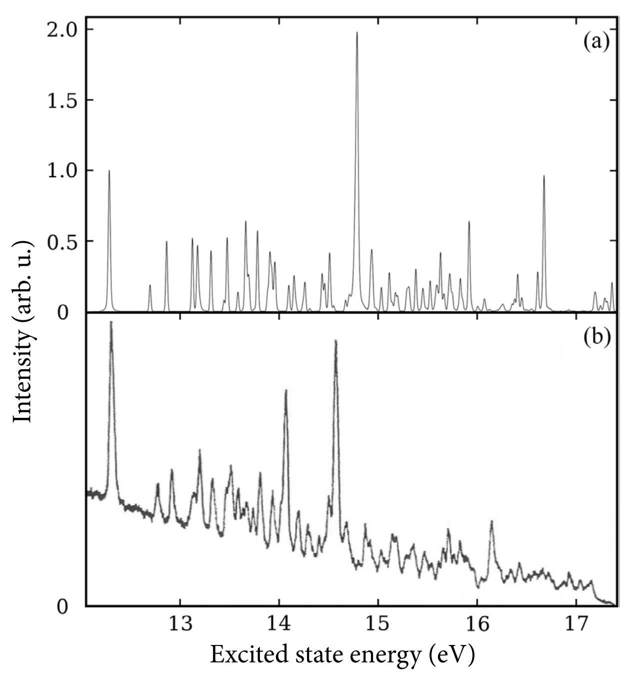

Figure. Calculated (a) and experimental [12] (b) ejected-electron spectrum of Cs atoms excited by 30 eV impacting electrons.

Table 1. Excitation energies E_{FAC} and E_{exp} [12] in eV, cross sections σ (10^{-18} cm^2) of Cs $5p^5nl(L_1S_1)n'l'\ LSJ$ states excited by 30 eV electrons (all energy levels up to 15.451 eV).

$nl(L_1S_1)n'l'\ LSJ$	E_{FAC}	E_{exp}	σ	$nl(L_1S_1)n'l'\ LSJ$	E_{FAC}	E_{exp}	σ
$6s^2\ ^2P_{3/2}$	12.289	12.307	9.88	$5d(^3F)6p\ ^4G_{7/2}$	14.787		0.02
$5d(^3P)6s\ ^4P_{1/2}$	12.700	12.786	1.38	$5d(^3D)6s\ ^2D_{3/2}$	14.790	14.574	19.7
$5d(^3P)6s\ ^4P_{3/2}$	12.867	12.930	3.60	$5d(^3P)6p\ ^2D_{3/2}$	14.794		0.05
$5d(^3P)6s\ ^4P_{5/2}$	13.127	13.149	3.05	$5d(^3P)6p\ ^4D_{7/2}$	14.840		0.03
$6s(^3P)6p\ ^4S_{3/2}$	13.128	13.011	0.68	$5d^2(^3F)\ ^4G_{7/2}$	14.852		0.04
$5d(^3F)6s\ ^4F_{9/2}$	13.178	13.204	2.88	$5d(^3F)6p\ ^2F_{7/2}$	14.854		0.01
$5d(^3P)6s\ ^2P_{1/2}$	13.193		1.87	$5d(^3P)6p\ ^4P_{5/2}$	14.883		0.04
$5d(^3F)6s\ ^4F_{7/2}$	13.315	13.344	3.12	$5d^2(^3P)\ ^4P_{3/2}$	14.927	15.055	1.99
$6s(^3P)6p\ ^4D_{7/2}$	13.446		0.57	$6s(^3P)6p\ ^2S_{1/2}$	14.940	14.950	3.36
$5d(^3F)6s\ ^4F_{5/2}$	13.477	13.484	2.68	$5d(^1D)6p\ ^2D_{5/2}$	14.981		0.10
$6s(^3P)6p\ ^4D_{5/2}$	13.480	13.600	1.18	$6s(^3P)7s\ 4P_{5/2}$	15.034		0.41
$6s(^3P)6p\ ^2D_{3/2}$	13.586	13.651	1.00	$5d^2(^3P)\ ^4P_{1/2}$	15.035	15.111	0.84
$5d(^3F)6s\ ^4F_{3/2}$	13.664	13.526	3.52	$5d(^3F)6p\ ^4D_{7/2}$	15.041		0.02
$5d(^3F)6s\ ^2F_{7/2}$	13.668	13.756	1.85	$5d(^3F)6p\ ^4G_{5/2}$	15.057		0.00
$5d(^3P)6s\ ^2P_{3/2}$	13.687	13.689	0.82	$5d^2(^3F)\ ^4F_{9/2}$	15.114		0.06
$5d(^1D)6s\ ^2D_{5/2}$	13.698		1.46	$6s(^3P)7s\ ^2P_{3/2}$	15.117		1.96
$6s(^1P)6p\ ^2P_{1/2}$	13.752		0.11	$5d(^3F)6p\ ^4F_{9/2}$	15.126		0.00
$5d(^3D)6s\ ^4D_{7/2}$	13.784	13.825	4.32	$5d(3P)7s\ ^2P_{1/2}$	15.128		0.19
$6s(^3P)6p\ ^4P_{5/2}$	13.887	13.952	0.11	$5d(^3F)6p\ ^4D_{5/2}$	15.138		0.03
$6s(^1P)6p\ ^2D_{3/2}$	13.908		0.81	$5d^2(^1D)\ ^2D_{5/2}$	15.144		0.40
$5d(^3D)6s\ ^2D_{5/2}$	13.909	14.043	2.05	$5d^2(^1D)\ ^2F_{7/2}$	15.153		0.04
$6s(^1P)6p\ ^2S_{1/2}$	13.928		1.94	$5d(^3P)7s\ ^4P_{3/2}$	15.177	15.171	0.90
$5d^2(^3F)\ ^4D_{1/2}$	13.959	14.072	3.22	$5d(^1D)6p\ ^2D_{3/2}$	15.182		0.07
$5d^2(^3F)\ ^4D_{3/2}$	14.100		1.50	$5d(^3P)7s\ ^4P_{1/2}$	15.198	15.211	0.74
$5d(^3P)6p\ ^4D_{1/2}$	14.153	14.310	1.87	$5d(^3F)6p\ ^4F_{7/2}$	15.203		0.00
$5d(^3P)6p\ ^2P_{3/2}$	14.172		0.42	$5d^2(^3F)\ ^2G_{7/2}$	15.205		0.08
$6s(^3P)6p\ ^2D_{5/2}$	14.244		0.50	$5d(^3D)6p\ ^4P_{3/2}$	15.243		0.02
$5d^2(^3F)\ ^4D_{5/2}$	14.263	14.427	1.45	$5d^2(^3P)\ ^2D_{5/2}$	15.289		0.42
$5d(^3P)6p\ ^4D_{3/2}$	14.312		0.14	$5d^2(^3P)\ ^2S_{1/2}$	15.290		0.12
$6s^2\ ^2P_{1/2}$	14.437	14.208	2.06	$5d(^1D)6p\ ^2F_{7/2}$	15.292		0.00
$5d^2(^3F)\ ^4D_{7/2}$	14.462	14.476	1.40	$5d^2(^3P)\ ^4S_{3/2}$	15.296	15.314	0.52
$5d(^3P)6p\ ^4P_{1/2}$	14.512	14.519	3.71	$5d(^3P)6p\ ^2S_{1/2}$	15.306		0.51
$5d(^3P)6p\ ^4D_{5/2}$	14.553		0.25	$5d^2(^3P)\ ^4D_{7/2}$	15.316	15.375	0.78
$5d^2(^3F)\ ^4G_{11/2}$	14.638		0.00	$5d(^1D)6p\ ^2F_{5/2}$	15.321		0.13
$5d(^3P)6p\ ^2P_{1/2}$	14.672	14.705	0.49	$5d(^3F)6p\ ^2G_{9/2}$	15.330		0.00
$5d(^3F)6p\ ^4G_{11/2}$	14.677		0.00	$5d(^3D)6p\ ^2P_{3/2}$	15.341		0.03
$5d(^3P)6p\ ^4P_{3/2}$	14.707		0.03	$5d^2(^1G)\ ^2H_{11/2}$	15.348		0.00
$5d^2(^1G)\ ^2F_{5/2}$	14.707		0.22	$5d(^3F)6p\ ^4F_{5/2}$	15.358		0.00
$5d(^3F)6p\ ^4G_{9/2}$	14.709		0.00	$5d(^3D)6s\ ^4D_{5/2}$	15.382	15.399	1.12
$5d^2(^3P)\ ^2P_{3/2}$	14.716		0.57	$5d(^3D)6s\ ^4D_{3/2}$	15.383		0.98
$5d^2(^3F)\ ^4G_{9/2}$	14.721		0.02	$5d(^1D)6p\ ^2P_{1/2}$	15.402		0.07
$5d^2(^3P)\ ^4P_{5/2}$	14.771		0.25	$6s(^3P)7p\ ^4S_{3/2}$	15.429		0.08
$5d(^1P)6s\ ^2P_{1/2}$	14.771	14.893	8.29	$5d^2(^3F)\ ^4F_{5/2}$	15.451	15.486	1.03

Table 2. Excitation energies E_{FAC} and E_{exp} [12] in eV, cross sections σ (10^{-18} cm^2) of Cs $5p^5nl(L_1S_1)n'l'$ *LSJ* states excited by 30 eV electrons (all energy levels with $\sigma \geq 5 \times 10^{-20}$ cm^2 from 15.463 up to 17.365 eV).

$nl(L_1S_1)n'l'$ *LSJ*	E_{FAC}	E_{exp}	σ	$nl(L_1S_1)n'l'$ *LSJ*	E_{FAC}	E_{exp}	σ
$5d^2(^3F)\,^4F_{3/2}$	15.463	15.521	0.35	$5d(^3F)7p\,^2D_{5/2}$	15.875		0.08
$6s(^3P)7p\,^4D_{7/2}$	15.474		0.05	$6s(^3P)7p\,^4P_{1/2}$	15.919	16.177	4.43
$5d(^3P)7p\,^4D_{1/2}$	15.487		0.06	$5d(^1F)7s\,^2F_{5/2}$	15.919		0.10
$6s(^3P)7p\,^2D_{5/2}$	15.490		0.09	$5d(^3F)7s\,^4F_{7/2}$	15.946		0.06
$6s(^3P)6d\,^4D_{7/2}$	15.526	15.575	1.43	$5d(^3P)7s\,^4P_{5/2}$	15.948		0.13
$6s(^3P)6p\,^4D_{1/2}$	15.535		0.21	$5d(^3P)8s\,^4P_{3/2}$	15.951		0.05
$5d(^3P)7p\,^4P_{1/2}$	15.562		0.10	$5d(^3P)8s\,^2P_{1/2}$	15.960		0.07
$6s(^3P)6d\,^2F_{7/2}$	15.577		0.18	$5d^2(^1G)\,^2F_{7/2}$	16.004		0.12
$6s(^3P)6d\,^4F_{9/2}$	15.582		0.17	$5d(^3F)6d\,^2P_{3/2}$	16.009	16.270	0.13
$6s(^3P)6d\,^4P_{1/2}$	15.583		0.10	$6s(^3P)8p\,^2D_{5/2}$	16.022		0.06
$5d(^3D)6p\,^2D_{3/2}$	15.588		0.05	$6s(^1P)7p\,^2P_{1/2}$	16.070		0.06
$6s(^3P)6d\,^4D_{3/2}$	15.590		0.36	$5d(^3D)7s\,^4D_{3/2}$	16.075	16.389	0.81
$6s(^3P)6d\,^4D_{5/2}$	15.591		0.26	$6s(^3P)8p\,^4S_{3/2}$	16.126	16.340	0.09
$6s(^3P)6d\,^2D_{5/2}$	15.599	15.655	0.69	$6s(^1P)6d\,^2D_{5/2}$	16.194		0.05
$5d(^3P)6d\,^4F_{3/2}$	15.609		0.09	$6s(^1P)6d\,^2F_{5/2}$	16.196		0.18
$6s(^3P)6p\,^4P_{3/2}$	15.611		0.33	$5d(^3F)6d\,^4D_{7/2}$	16.212		0.05
$5d(^3P)7p\,^4D_{5/2}$	15.619		0.07	$5d(^3P)7s\,^4P_{3/2}$	16.232		0.13
$5d(^1F)6s\,^2F_{7/2}$	15.631	15.689	2.40	$5d(^1D)7s\,^2D_{3/2}$	16.245		0.10
$6s(^3P)6d\,^2P_{1/2}$	15.632	15.742	0.38	$6s(^1P)6d\,^2P_{1/2}$	16.251		0.06
$5d(^3D)7p\,^4D_{1/2}$	15.637		0.17	$6s(^1P)6d\,^2D_{3/2}$	16.258		0.06
$5d(^3P)6d\,^2F_{5/2}$	15.641		0.12	$6s(^3P)6p\,^2P_{3/2}$	16.269	16.458	0.31
$5d(^3P)6d\,^4D_{3/2}$	15.644		0.06	$5d(^3P)6d\,^2F_{7/2}$	16.344	16.563	0.08
$5d(^3P)6d\,^4F_{7/2}$	15.658		0.11	$5d(^3P)6d\,^4P_{1/2}$	16.359	16.610	0.24
$5d(^3P)6d\,^4P_{5/2}$	15.662		0.17	$5d(^1P)6p\,^2P_{1/2}$	16.411	16.696	2.04
$6s(^3P)6d\,^2D_{3/2}$	15.665	15.801	0.31	$4f(^1F)6s\,^2F_{5/2}$	16.429	16.674	0.07
$5d(^3P)6d\,^4D_{1/2}$	15.665		0.16	$5d(^3D)6p\,^4P_{1/2}$	16.452	16.758	0.64
$6s(^3P)6p\,^4D_{3/2}$	15.670		0.18	$5d(^1D)6d\,^2P_{3/2}$	16.571	16.806	0.16
$5d(^3P)6d\,^4F_{5/2}$	15.676		0.12	$6s(^1P)8s\,^2P_{1/2}$	16.573	16.910	0.19
$6s(^1P)7s\,^2P_{3/2}$	15.711		0.33	$5d(^1D)7p\,^2P_{1/2}$	16.612	16.968	1.98
$5d(^3D)6p\,^4P_{5/2}$	15.713		0.28	$5d(^3D)6d\,^4P_{1/2}$	16.656		0.07
$5d(^3F)6s\,^2F_{5/2}$	15.723	15.853	1.20	$6s(^3P)6p\,^4P_{1/2}$	16.676	16.998	7.97
$6s(^3P)7p\,^4P_{3/2}$	15.727		0.25	$5d(^3D)6d\,^4P_{3/2}$	16.676		0.12
$6s(^1P)7s\,^2P_{1/2}$	15.732		0.64	$5d(^1D)8s\,^2D_{3/2}$	16.722		0.13
$6s(^1P)6p\,^2D_{5/2}$	15.750	15.996	0.80	$6s(^1P)7d\,^2P_{3/2}$	16.742		0.10
$5d(^3P)6d\,^2P_{3/2}$	15.761		0.07	$6s(^1P)8d\,^2P_{3/2}$	17.082		0.09
$5d(^3F)7s\,^4F_{9/2}$	15.778		0.09	$6s(^3P)9s\,^4P_{1/2}$	17.191		0.41
$5d^2(^3P)\,^2D_{3/2}$	15.811		0.20	$5d(^3P)7d\,^2P_{1/2}$	17.204	17.030	0.67
$5d^2(^1S)\,^2P_{3/2}$	15.834	15.922	1.57	$6s(^3P)9s\,^2P_{1/2}$	17.248		0.08
$5d(^3F)7s\,^2F_{7/2}$	15.839		0.08	$5d(^3F)6p\,^4D_{1/2}$	17.251	17.080	0.20
$6s(^3P)8s\,^4P_{5/2}$	15.844		0.19	$6s(^3P)9s\,^4P_{3/2}$	17.288	17.148	0.43
$6s(^3P)7p\,^2S_{1/2}$	15.852	16.076	0.24	$5d(^3D)7s\,^4D_{1/2}$	17.294		0.39
$5d^2(^3F)\,^2D_{5/2}$	15.859		0.22	$5d(^1P)7s\,^2P_{3/2}$	17.365	17.186	1.49

Table 3. Revised Table 2 [11] classification of the $5p^5nl(L_1S_1)n'l'$ *LSJ* states of Cs. A possible unambiguous assignment is presented in the brackets.

Previous [11]	Present		Previous [11]	Present
$6s(^1P)6p\ ^2D_{3/2}$	$6s(^3P)6p\ ^2D_{3/2}$		$5d(^3F)6s\ ^4F_{3/2}$	$5d2(^3P)\ ^4S_{3/2}$
$5d(^1D)6s\ ^1D_{3/2}$	$5d(^3F)6s\ ^4F_{3/2}$	$(5d(^1D)6s\ ^2D_{3/2})$	$5d(^1F)6s\ ^2F_{5/2}$	$5d(^3F)6s\ ^2F_{5/2}$
$6s(^3P)6p\ ^2P_{3/2}$	$6s(^1P)6p\ ^2D_{3/2}$	$(6s(^3P)6p\ ^2P_{3/2})$	$6s(^3P)7s\ ^2P_{1/2}$	$6s(^1P)7s\ ^2P_{1/2}$
$5d(^1P)6s\ ^2D_{3/2}$	$5d(^3D)6s\ ^2D_{3/2}$	$(5d(^1P)6s\ ^2P_{3/2})$	$5d(^3D)7p\ ^2P_{1/2}$	$5d(^1D)6p\ ^2P_{1/2}$
$6s(^3P)7s\ ^4P_{3/2}$	$6s(^3P)7s\ ^2P_{3/2}$		$6s(^3P)7d\ ^2P_{1/2}$	$6p^2(^3P)\ ^2P_{1/2}$
$6s(^3P)7s\ ^2P_{3/2}$	$5d(^3P)7s\ ^4P_{3/2}$		$6s(^1P)6d\ ^2P_{1/2}$	$5d(^3D)6d\ ^2S_{1/2}$
$6s(^1P)7p\ ^2S_{1/2}$	$5d(^3P)6p\ ^2S_{1/2}$	$(5d(^3D)6p\ ^2P_{1/2})$		

Table 4. The factors $1 + \Sigma_{K>0,\mathrm{even}} A_K\alpha_K P_K(\cos\theta)$ for the $5p^5nln'l'$ J states of Cs at 30 eV energy of impacting electrons.

	$6s^2$	5d6s			6s6p	
θ J	3/2	3/2	5/2	7/2	3/2	5/2
0°	1.27	1.48	2.31	2.88	1.22	1.47
15°	1.24	1.43	2.07	2.35	1.20	1.37
30°	1.17	1.30	1.52	1.40	1.14	1.16
45°	1.07	1.12	1.00	0.90	1.06	0.97
54.7°	1.00	1.00	0.81	0.85	1.00	0.91
75°	0.97	0.81	0.75	0.77	0.91	0.93
90°	0.89	0.76	0.78	0.68	0.89	0.96

4. Conclusions

Excitation energies of the $5p^5nln'l'$ *jjJ* autoionizing states of Cs were obtained in the large scale configuration interaction and Dirac–Fock–Slater approximations. The *LSJ* coupling scheme of angular momenta was used for classification of these states. The values of level energies and simulated Auger electron emission spectra for 30 eV impacting electrons taking into account the asymmetry of the angular distribution of emitted Auger electrons were used for identification of the experimental spectrum measured at 75° with respect to the direction of impacting electrons [12]. The intensity of the lines of Auger electrons from the states with $J > {}^1/_2$ could decrease up to 25% at the angle of 75° with respect to the $J = {}^1/_2$ states. The largest intensities were obtained for the quartet and other dipole-forbidden lines as the 30 eV energy of impacting electrons is close to the 5p-core excitation threshold. Excitation cross sections for the dipole-allowed transitions achieve maximum values at higher impacting electron energies. New quantum numbers were assigned to 27 of 63 experimental lines observed in [12]. A full identification of 63 lines of [12] was performed. To perform a more robust identification of the doublet states, the experimental spectra within 50–70 eV energy of impacting electrons is desirable. A complete identification of the $5p^5nln'l'$ J states of the Cs I spectrum is possible if higher resolution and wider energy range experimental spectra are performed.

Acknowledgements

This research was performed under the Project VP1-3.1-ŠMM-07-K-02-013 funded by the European Social Fund under the Global Grant measure.

References

[1] A. Kupliauskienė, P. Bogdanovich, and A. Borovik, Radiative transitions between lowest autoionizing states in sodium, Lith. J. Phys. **47**(1), 7–13 (2007), http://dx.doi.org/10.3952/lithjphys.47108

[2] A. Borovik and A. Kupliauskienė, On cascade transitions between autoionizing doublet levels in sodium, Phys. Scripta **77**(5), 055301 (2008), http://dx.doi.org/10.1088/0031-8949/77/05/055301

[3] A.E. Kramida, Revised interpretation of the Na I EUV absorption spectrum, J. Phys. B **43**(20), 205001 (2010), http://dx.doi.org/10.1088/0953-4075/43/20/205001

[4] A. Borovik, A. Kupliauskienė, and O. Zatsarinny, Excitation-autoionization cross section of alkali atoms by electron impact, J. Phys. B **46**(21), 215201 (2013), http://dx.doi.org/10.1088/0953-4075/46/21/215201

[5] A. Kupliauskienė, P. Bogdanovich, A.A. Borovik, O. Zatsarinny, A.N. Grum-Grzhimailo, and K. Bartschat, The role of cascade processes in electron-impact excitation of the $(3p^54s^2)$ $^2P_{3/2,1/2}$ autoionizing levels in potassium, J. Phys. B **39**(3), 591–601 (2006), http://dx.doi.org/10.1088/0953-4075/39/3/012

[6] A. Borovik, V. Roman, and A. Kupliauskienė, The $4p^6$ autoionization cross section of Rb atoms excited by low-energy electron impact, J. Phys. B **45**(4), 045204 (2012), http://dx.doi.org/10.1088/0953-4075/45/4/045204

[7] J.P. Connerade, Absorption spectrum of Cs I in the vacuum ultraviolet, Astrophys. J. **159**(2), 685–694 (1970), http://dx.doi.org/10.1086/150342

[8] J.P. Connerade, M.W.D. Mansfield, G.H. Newsom, D.H. Tracy, M.A. Baig, and K. Thimm, A study of 5p excitation in atomic barium I. The 5p absorption spectra of Ba I, Cs I and related elements, Phil. Trans. Roy. Soc. Lond. A **290**(1371), 327–352 (1979), http://dx.doi.org/10.1098/rsta.1979.0002

[9] A. Borovik and A. Kupliauskienė, The $5p^6$ autoionization cross section of cesium atoms: contribution to single ionization by electron impact, J. Phys. B **42**(16), 165202 (2009), http://dx.doi.org/10.1088/0953-4075/42/16/165202

[10] M.F. Gu, The flexible atomic code, Can. J. Phys. **86**(5), 675–689 (2008), http://dx.doi.org/10.1139/p07-197

[11] A. Kupliauskienė, Theoretical study of the $5p^5nln'l'$ autoionizing states of Cs, Phys. Scripta **84**(4), 045304 (2011), http://dx.doi.org/10.1088/0031-8949/84/04/045304

[12] V. Pejčev and K.J. Ross, High-resolution ejected-electron spectrum of caesium vapour autoionising levels excited by 30 to 400 eV electrons, J. Phys. B **10**(14), 2935–2941 (1977), http://dx.doi.org/10.1088/0022-3700/10/14/025

[13] A. Borovik, A. Kupliauskienė, and O. Zatsarinny, Excitation cross sections and spectroscopic classification of autoionizing levels in a caesium atom, J. Phys. B **44**(14), 145203 (2011), http://dx.doi.org/10.1088/0953-4075/44/14/145203

[14] A. Borovik, A. Kupliauskienė, and O. Zatsarinny, New spectroscopic classification of lowest autoionizing levels in Cs atoms, J. Phys. Conf. **388**(4), 042021 (2012), http://dx.doi.org/10.1088/1742-6596/388/4/042021

[15] A. Kupliauskienė, Atomic theory methods for the polarization in photon and electron interactions with atoms, Lith. J. Phys. **44**(3), 199–218 (2004), http://dx.doi.org/10.3952/lithjphys.44303

[16] A. Kupliauskienė, A general expression for the excitation cross-section of polarized atoms by polarized electrons, Phys. Scripta **75**(4), 524–530 (2007), http://dx.doi.org/10.1088/0031-8949/75/4/026

[17] A. Kupliauskienė and V. Tutlys, Application of graphical technique for Auger decay following photoionization of atoms, Phys. Scripta **67**(4), 290–300 (2003), http://dx.doi.org/10.1238/Physica.Regular.067a00290

[18] A. Kupliauskienė and G. Kerevičius, Theoretical study of the $4p^5nln'l'$ autoionizing states of Rb excited by electron impact, Phys. Scripta **88**(6), 065305 (2013), http://dx.doi.org/10.1088/0031-8949/88/06/065305

[19] O. Zatsarinny, 2011 [private communication].

[20] A.J. Mendelsohn, C.P.J. Barty, M.H. Sher, J.F. Young, and S.E. Harris, Emission spectra of quasimetastable levels of alkali-metal atoms, Phys. Rev. A **35**(5), 2095–2101 (1987), http://dx.doi.org/10.1103/PhysRevA.35.2095

[21] A. Kupliauskienė and V. Tutlys, Properties of Auger electrons following excitation of polarized atoms by polarized electrons, Nucl. Instrum. Methods B **267**(2), 263–265 (2009), http://dx.doi.org/10.1016/j.nimb.2008.10.039

[22] A. Kupliauskienė, Fluorescence of polarized atoms excited by polarized electrons, Nucl. Instrum. Methods B **267**(2), 266–269 (2009), http://dx.doi.org/10.1016/j.nimb.2008.10.038

[23] S. Kaur and R. Srivastava, Excitation of the lowest autoionizing $np^5(n+1)s^2,{}^2P_{3/2,1/2}$ states of Na($n = 2$), K($n = 3$), Rb($n = 4$) and Cs($n = 5$) by electron impact, J. Phys. B **32**(10), 2323–2342 (1999), http://dx.doi.org/10.1088/0953-4075/32/10/303

[24] C.F. Fischer, General Hartree-Fock program, Comput. Phys. Comm. **43**(3), 355–365 (1987), http://dx.doi.org/10.1016/0010-4655(87)90053-1

SUŽADINTŲ 30 eV ELEKTRONAIS Cs ATOMO $5p^5nln'l'$ *LSJ* ENERGIJOS LYGMENŲ KLASIFIKACIJA

G. Kerevičius, A. Kupliauskienė

Vilniaus universiteto Teorinės fizikos ir astronomijos institutas, Vilnius, Lietuva

Santrauka

Cs atomo $5p^5nln'l'$ autojonizacinių konfigūracijų lygmenų energijos, autojonizacijos tikimybės ir sužadinimo elektronais skerspjūviai apskaičiuoti taikant konfigūracijų superpozicijos metodą. Į reliatyvistines pataisas atsižvelgta ieškant radialiųjų banginių funkcijų Dirako, Foko ir Sleiterio artinyje. Banginės funkcijos, transformuotos iš *jjJ* į *LSJ* judesio kiekio momentų jungimo ryšį, panaudotos teoriniams energijos lygmenims klasifikuoti. Apskaičiuoti duomenys panaudoti Cs atomo, sužadinto 30 eV elektronais, Ožė elektronų intensyvumų spektrui modeliuoti. Modeliuojant spektrą atsižvelgta į Ožė elektronų kampinio pasiskirstymo priklausomybę nuo registravimo kampo. Pastebėta, kad esant 75° registravimo kampui šuolių iš $J > {}^1/_2$ būsenų linijų intensyvumai yra iki 25 % mažesni nei $J = {}^1/_2$ atveju. Sumodeliuotas spektras panaudotas eksperimentinio spektro, išmatuoto 75° kampu 30 eV energijos žadinančių elektronų krypties atžvilgiu, linijoms identifikuoti. Nustatyta, kad 30 eV energijos žadinančių elektronų atveju didžiausi intensyvumai yra šuoliams iš kvartetinių ir kitų dipoliniame artinyje draustinų būsenų, nes ši energijos vertė yra artima 5p sluoksnio sužadinimo slenksčiui. Norint patikimiau identifikuoti dubletines būsenas, reikalingi nauji eksperimentai, kur žadinančių elektronų energija lygi 50–70 eV ir būtų išmatuotas platesnio intervalo spektras. Eksperimentiniame spektre yra nemažai persiklojusių linijų, taigi reikalingi didesnės skiriamosios gebos spektrai.